A Super-Lyophobic 3D PDMS Channel as a Novel Microfluidic Platform to Manipulate Oxidized Galinstan®

Daeyoung Kim, Dong-Weon Lee, Wonjae Choi, Jeong-Bong (JB) Lee, Senior Member, IEEE

***Abstract*— We report a 3D super-lyophobic polydimethylsiloxane (PDMS) microfluidic channel patterned with an array of multi-scale surface texture as a novel microfluidic platform to mobilize naturally oxidized Galinstan®. Galinstan® is a liquid metal that has multiple advantages over mercury such as non-toxicity, higher thermal conductivity, and lower electrical resistivity. However, Galinstan® gets easily oxidized in air environment and it becomes a viscoelastic liquid that wets almost any solid surface. We studied the feasibility of developing super-lyophobic surfaces against Galinstan®, using various flat and textured surfaces including PDMS micro pillar and micro ridge arrays by measuring static and dynamic contact angles. The highest advancing angle of 175º and receding angle of 163º were achieved on a surface patterned with micro pillars each of which was textured with additional roughness. Pitch distance between pillars was 175 μm. An extremely simple PDMS-PDMS bonding technique was used to fabricate a 3D super-lyophobic channel structure as a microfluidic platform for oxidized Galinstan® droplets. The driving force to actuate a ~3 μL Galinstan® droplet in the 3D super-lyophobic channel was 3.11 ± 0.23 mN.**

***Index Terms*—Liquid metal, Galinstan®, 3D PDMS channel, Super-lyophobicity, Microfluidic platform.**

I. INTRODUCTION

Gallium-based non-toxic metal eutectic alloys are in liquid phase at room temperature. As an alternative to toxic mercury, gallium-based metal eutectic alloys have been investigated for various applications including microsyringe for biology [1], radio frequency (RF) switch [2], magnetohydrodynamic (MHD) pump [3], heat transfer [4], current limiter [5], and tunable frequency selective surface (FSS) [6] among others. Although it has great potential for a variety of applications, gallium-based liquid metal alloys has not been widely used because of the fact that they instantly oxidize in air environment and the metal alloy behaves like a viscoelastic gel. Furthermore, viscous oxide surface skin of gel-like gallium-based liquid metal alloys is known to adhere to almost any surface [7]. This instant oxidation is a difficult problem to overcome and device development using gallium-based liquid alloys has slowed down considerably.

Multiple methods to remove the oxide layer have been reported but they have only limited applicability: it was reported that Galinstan® (Geratherm Medical AG, Geschwenda, Germany), a commercially available ternary gallium-based liquid metal alloy, behaves like a simple liquid in the below 1 ppm of oxygen environment [8]. This requires, however, a very tight hermetic packaging for the microfluidic platform for Galinstan®. It was also shown that either diluted hydrochloric acid (HCl) solution or HCl vapor can remove oxide skin in eutectic Ga-based alloy [9, 10]. However, the usage of HCl may not be applicable for many applications.

Removal of the viscous oxide surface skin of gallium-based liquid metal alloys may be crucial for certain applications like micro switches, where the existence of a layer with high electrical resistance can compromise the performance of the device. However, in other applications such as heat transfer, MHD pump and FSS, increased electrical resistance at the surface is not a critical issue. If there is a simple but universally applicable method that makes oxide surface skin does not adhere to surrounding surfaces, it may unleash unexplored potential applications of the gallium-based liquid metal alloy-based devices, especially in the field of microfluidics.

Although there have been countless literatures on super-hydrophobic surfaces [11-14], to the best of our knowledge, there was no published report on super-lyophobic surface in air environment for gallium-based liquid metal alloys, probably due to the strong wettability of the gallium-based alloys. In this paper, we report our study on the lyophobicity against the naturally oxidized Galinstan®, using i) flat surfaces with different surface chemistry, and ii) multiple surfaces with different surface textures such as an array of PDMS-based micro pillars and ridges. We also describe an extremely simple method of fabricating a 3D super-lyophobic channel with the textured inner surface as a microfluidic platform for the oxidized Galinstan®.

II. LYOPHOBICITY OF VARIOUS FLAT SURFACES

Initially, we have studied various flat surfaces (PDMS, SU8, SiO_2, and glass) with different lyophobic coatings (Teflon®,

Manuscript received April 2, 2013. This work was supported in part by World Class University (WCU) project (R32-2009-000-20087-0) funded by Korean government. The authors would like to thank UTD clean room staff for their support on this work.

D. Kim and J.-B. Lee are with the Department of Electrical Engineering, The University of Texas at Dallas, Richardson, TX 75080 USA (e-mail: daeyoung@utdallas.edu; jblee@utdallas.edu).

D-W Lee is with the School of Mechanical Systems Engineering, Chonnam National University, Gwangju, 550-757 South Korea (e-mail : mems@chonnam.ac.kr)

W. Choi is with the Department of Mechanical Engineering, The University of Texas at Dallas, Richardson, TX 75080 USA (e-mail: wxc111930@utdallas.edu).

Cytop, and fluorocarbon (FC) polymer) on their lyophobic characteristics for the oxidized Galinstan® droplet. All Galinstan® droplets studied in this paper were dispensed through a pipette and oxidized instantly at atmospheric room temperature environment. To quantify the lyophobicity, we measured advancing and receding angles of oxidized Galinstan® using a goniometer (Ramé-hart 260-F4) on the following flat substrates: 18 μm thick PDMS on a glass, a bare soda lime glass slide (Corning Life Science), 10 μm thick SU-8 on a silicon (Si) wafer, and 2 μm thick thermally grown SiO_2 on a Si wafer. Optionally, one of the following layers was deposited to improve the surface lyophobicity: 30 nm thick Teflon®, 1 μm thick Cytop, 20 nm fluorocarbon (FC - C_xF_y) polymer. For the PDMS substrate, RTV 615 A and B (HISCO Inc.) were mixed in 10:1 ratio and the PDMS was spin coated on a wafer and cured at room temperature for one day. The Teflon® and Cytop were spin coated and the FC polymer coating was obtained by applying inductively coupled plasma power with a mixture of fluorocarbon precursors C_4F_8 and Ar gas.

The relationship between sliding angle, advancing and receding contact angle are given by [15]:

$$\frac{mg\sin\alpha}{w} = \gamma_{LG}(\cos\theta_{rec} - \cos\theta_{adv}) \qquad (1)$$

where g is the gravitational acceleration, m is the mass of the droplet, w is the dimension of the droplet at the contact surface, α is the sliding angle, and θ_{rec} and θ_{adv} are receding and advancing contact angles, respectively. Therefore, the contact angle hysteresis, difference between the advancing and receding contact angles, should be small to achieve small sliding angle.

The volume of the Galinstan® droplet was modulated by using a pipette with Teflon®-coated tip (inner diameter of 0.3 mm) while the side view of the droplet was recorded by charge-coupled device (CCD) camera at 70 frames per second. The advancing and receding contact angles were obtained from the frame of the recorded movie just before the contact line began to move. The advancing angles of various flat surfaces are shown in Table I.

Table I. Advancing contact angles of oxidized Galinstan® droplet on various flat surfaces

Substrates	No coating	Teflon®	Cytop	FC polymer
PDMS	151.5	160.0	159.5	164.0
SU8	146.0	159.5	154.0	158.0
SiO_2	140.5	157.3	159.5	159.5
Glass	143.5	155.0	158.0	161.0

Among four materials studied, the bare PDMS surface is well known for its inherent hydrophobicity with static water contact angle of 120º [16], distinguishably higher than those of other three materials. Although general lyophobicity is different from hydrophobicity, the bare PDMS surface showed the highest advancing angle. Surfaces coated with hydrophobic materials (Teflon®, Cytop and FC polymer) also showed improvement in advancing angles on all surfaces. Among them, the FC polymer-coated PDMS showed the highest advancing angle of 164° (Fig.1a). High advancing contact angle, however, does not guarantee that the surface is lyophobic; except the FC polymer-coated PDMS surface on which the receding contact angle was measured to be 39° (Fig.1b), the receding contact angles of all other surfaces were less than 10° resulting in high contact angle hystereses. After the receding of the naturally oxidized Galinstan® droplet on these various flat surfaces, residue of oxidized Galinstan® remained on the surface even for the FC polymer-coated PDMS surface (Fig.1c). Therefore, it turned out that certain surface modification on these substrates is necessary to develop a microfluidic platform for residue-free, on-demand manipulation of naturally oxidized Galinstan® droplet.

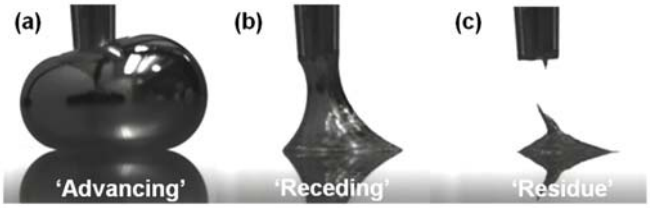

Fig. 1. Advancing angle (164°), receding angle (39°), and residue of oxidized Galinstan® on the FC polymer-coated PDMS surface.

III. Lyophobicity of PDMS micro arrays

Based on the results from flat surfaces, we selected PDMS as our base material for subsequent studies. PDMS also has very well-known unique characteristics such as outstanding replication characteristics down to the length-scale of sub-micrometer [17], physical flexibility due to its extremely low Young's modulus (< 4 MPa) [18], and high optical transparency throughout the ultraviolet and visible wavelengths [19].

To improve lyophobicity, we first tested two types of surface textured PDMS micro arrays: micro pillar arrays and micro ridge arrays. Vertical height of all PDMS micro textures was designed to be 45 μm. The fabrication of PDMS micro pillar and micro ridge arrays started with spin coating of SU-8 2025 photoresist (PR) (MicroChem Corp.) on a thermally grown oxidized Si wafer to get approximately 45μm thick PR. The PR was soft-baked on the hot plate at 65°C for 2min, 95°C for 3 min, and finally 65°C for 2 min. Then, an UV exposure dose of 140 mJ/cm^2 is applied by standard photolithography to create an inverse pattern of target structure, and finally a post bake was applied with a same temperature and time of soft bake. Finally, it was developed in SU-8 developer (propylene glycol methyl ether acetate) for 3 min under gentle stirring condition, and was cleaned with isopropyl alcohol and DI water (Fig. 2a). After developing, the PDMS was casted over the PR mold it was cured at room temperature for a day to have flexible characteristics (Fig. 2b). After curing, PDMS peeled off from the mold and it replicated arrays (Fig. 2c). 80 nm thick FC polymer was deposited on top of the PDMS arrays to enhance lyophobicity (Fig. 2d).

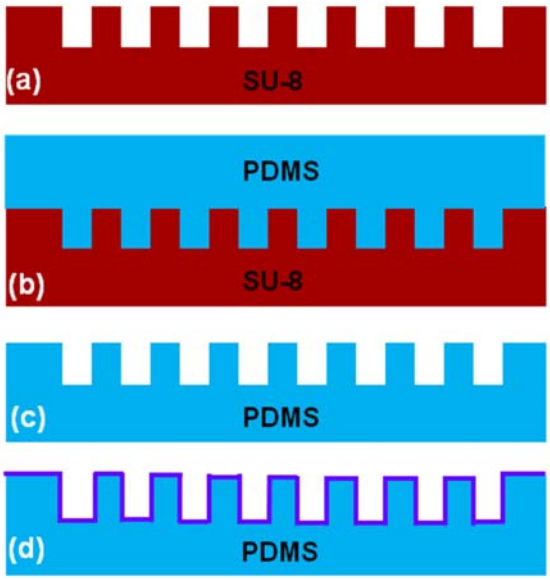

Fig. 2. Fabrication sequence of the super-lyophobic micro textured PDMS surfaces: (a) patterned SU-8 mold, (b) PDMS casting, (c) replicated PDMS, (d) FC polymer deposition on the replicated PDMS micro arrays.

PDMS micro pillar arrays had various dimensions including 25 μm pillar diameter 25 μm gap, 75 μm diameter 25 μm gap, 75 μm diameter 100 μm gap, 75 μm diameter 150 μm gap, 75 μm diameter 200 μm gap, and 75 μm diameter 250 μm gap. PDMS micro ridge arrays had various widths and gaps (25 μm width 25 μm gap, 75 μm width 25 μm gap, 75 μm width 100 μm gap, 75 μm width 150 μm gap, 75 μm width 200 μm gap). Fig. 3 shows scanning electron microscope (SEM) images of the micro pillar arrays (Fig. 3a and b) and micro ridge arrays (Fig. 3c and d).

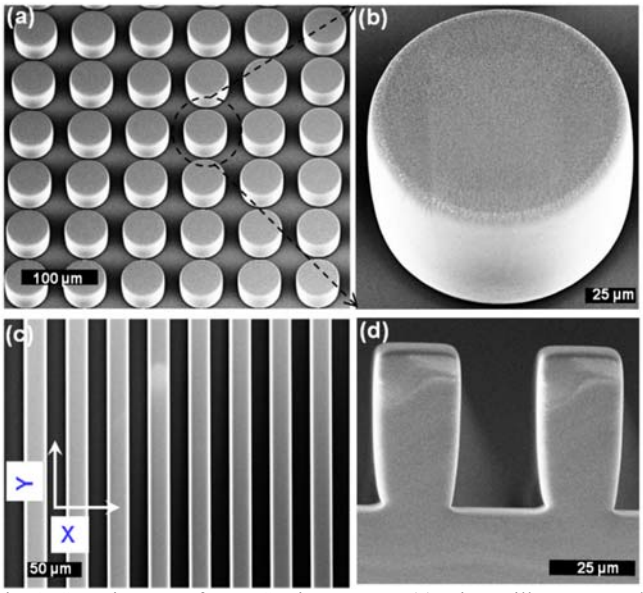

Fig. 3. SEM images of PDMS micro arrays: (a) micro pillar array and (b) a close-up 15° tilted view of a micro pillar, (c) micro ridge array and (d) a close-up side view of micro ridges.

Lyophobicity of textured surfaces was studied by measuring static and dynamic contact angles. Fig. 4 shows the images of static droplets of 7.8 μL oxidized Galinstan® on micro pillar arrays with the same pillar diameter (75 μm) but with various gap distances. Galinstan® droplet is not spherical due to the viscoelastic oxidized layer on the surface. The droplet on a 225 μm pitch distance (75 μm diameter 150 μm gap) micro pillar array clearly formed a non-wetting Cassie state [19], confirmed by the presence of air pockets underneath the droplet (Fig. 4a). We observed the droplets on all micro pillar arrays with gap distances smaller than 150 μm formed a Cassie state, as it becomes more difficult for a Galinstan® to penetrate between micro pillars when the gap distance becomes smaller. On the other hand, the image of the Galinstan® droplet on a micro pillar array with 250 μm gap distance showed that the droplet penetrated between pillars, forming a fully wetted Wenzel state (Fig. 4c). We also found that the droplets on any micro pillar arrays with gap distance larger than 250 μm showed Wenzel state. There were intermediate transition states between the Cassie and the Wenzel states. Fig. 4b shows Galinstan® droplet on a 200 μm gap distance. The droplet penetrated into a portion of the texture, but we could observe some intact air pockets as well. It was also found that micro ridge arrays with gap distances smaller than 150 μm (75 μm ridge width) showed Cassie state. Table II shows static contact angles for various pitch distances in the range of 50 to 225 μm.

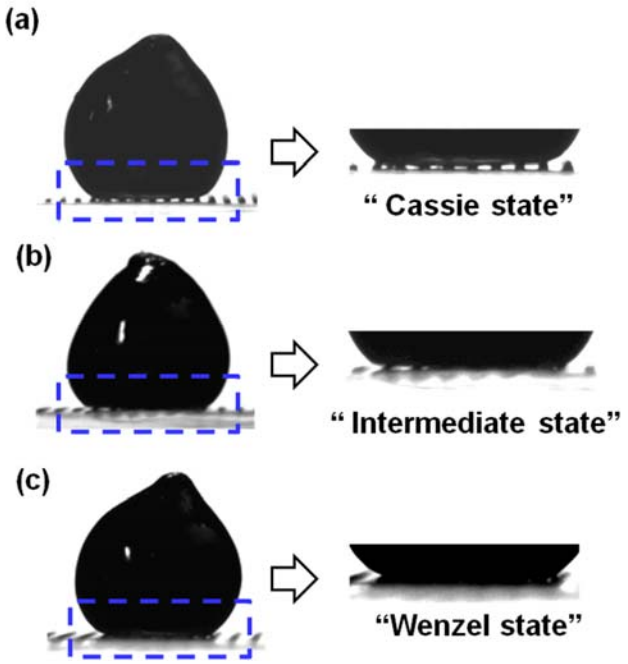

Fig. 4. A 7.8 μL oxidized Galinstan® droplet on (a) 150 μm gap micro pillar array, showing a non-wetting Cassie state, (b) 200 μm gap micro pillar array, showing an intermediate transition state, and (c) 250 μm gap micro pillar array (no air pockets), showing a fully-wetted Wenzel state. The diameter of all micro pillars is 75 μm.

Table II. Static contact angles for a 7.8 μL oxidized Galinstan® droplet on PDMS micro pillar and micro ridge arrays

Substrates	Diameter / width (μm)	Pitch distance (μm)	Solid fraction (f_s)	Static contact angle (°)
Micro pillar array	25	50	0.196	141.6 ± 0.2
	75	100	0.442	135.8 ± 1.2
		175	0.144	140.6 ± 3.5
		225	0.087	139.1 ± 4.4
Micro ridge array	25	50	0.500	139.5 ± 1.1
	75	100	0.750	131.4 ± 1.8
		175	0.429	133.5 ± 3.7
		225	0.334	137.9 ± 1.2

The static contact angle of a droplet in the Cassie state is represented by the following equation [20]:

$$\cos\theta_c = f_s(1+\cos\theta) - 1 \quad (2)$$

where f_s is the fraction of the solid in contact with the liquid and θ_c is the contact angle in Cassie state. Since the contact area of the micro pillar arrays is smaller than that of the micro ridge arrays for the same pitch distances, the static contact angle of the micro pillar arrays is relatively larger than that of the micro ridge arrays. The static contact angle of 139.1° on a pillar array with 75 μm diameter 150 μm gap distance (solid fraction = 0.087) is not remarkably high, considering the extremely low solid fraction, due to the highly hysteretic behavior of the oxidized Galinstan®.

The dynamic contact angles were measured in the same way as described in the previous section. Table III shows dynamic contact angles of the oxidized Galinstan® droplet on micro pillar arrays and micro ridge arrays with various dimensions. For the micro ridge arrays, contact angles were measured from two different viewing directions, when the droplet was advancing/receding i) across the ridges (X direction; see Fig. 3c) and ii) along the ridges (Y direction).

Table III. Dynamic contact angles of oxidized Galinstan® droplet

Substrates	Pitch distance (μm)	Solid fraction (f_s)	Dynamic contact angles (°)		Contact angle hysteresis (°)
			Adv.	Rec.	
Micro pillar array	50	0.196	179.0	75.3	103.7
	100	0.442	163.5	51.3	112.2
	175	0.144	160.5	77.9	82.6
	225	0.087	153.5	51.0	102.5
Micro ridge array (X direction, across the ridges)	50	0.500	161.0	50.0	111.0
	100	0.750	161.8	20.5	141.3
	175	0.429	161.5	43.3	118.2
	225	0.334	163.5	40.0	123.5
Micro ridge array (Y direction, along the ridges)	50	0.500	155.3	38.3	117.0
	100	0.750	156.8	16.8	140.0
	175	0.429	156.8	32.5	124.3
	225	0.334	158.3	37.0	121.3

For simple fluids such as water or hexadecane, the contact angle hysteresis when a droplet advances/recedes along the ridges (Y direction) is less than that on micro pillar arrays with the same solid fraction as, for micro pillar array, the solid fraction near the contact line significantly changes between advancing and receding droplets [21]. However, for Galinstan®, we found that the contact angle hystereses on the micro ridge arrays in both directions (X and Y) are larger than those on the micro pillar arrays. We suspect that the viscoelasticity of Galinstan® combined with its extreme wettability (see Fig. 1), causes the receding of the droplet from the top of pillars and ridges virtually impossible, leading to the discrepancy between the conventional model of hysteresis and the observed values. The pillar array with 75 μm diameter and 100 μm gap distance showed the smallest contact angle hysteresis (82.6°) among all textured surfaces. Nonetheless, the residue of oxidized Galinstan® was still left on the surface after receding, even though the droplet formed the Cassie state (Fig. 5).

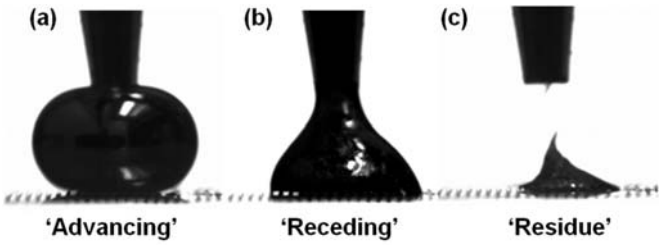

Fig. 5. Advancing angle (160.5°), receding angle (77.9°), and residual state of the oxidized Galinstan® on the micro pillar array with 75 μm diameter and 100 μm gap distance.

Although there was decrease in contact angle hysteresis from those of the various flat surfaces to the surfaces textured with PDMS micro arrays, it turned out that naturally oxidized Galinstan® droplet did not completely dewet from all tested surfaces regardless of the shape and pitch distance of the PDMS micro arrays.

IV. Lyophobicity of Multi-Scale Surface Textured PDMS Micro Pillar Arrays

It is known that the super-hydrophobicity of natural water-repellent surfaces stems from a combination of multi-scale surface texturing [22] and surface chemistry [23]. To further improve lyophobicity of the PDMS micro arrays, we further studied lyophobicity of multi-scale surface textured PDMS micro pillar arrays.

The fabrication of multi-scale surface textured PDMS micro pillar arrays started with triple-spin coating of AZP4620 photoresist (PR) (AZ Electronic materials) on a thermally oxidized Si wafer to get approximately 45μm thick PR. The PR was intentionally under-baked in a convection oven at 88 ºC (typical soft-bake temperature is 110°C on a hot plate). Then, the PR was under-exposed with the exposure dose of 800 mJ/cm^2 (typical exposure dose is > 1,600 mJ/cm^2) [24]. After developing of PR with diluted AZ400K (AZ Electronic materials) (Fig. 6a), the PDMS was casted over the PR mold and it was cured at room temperature for one day (Fig. 6b). The replicated PDMS showed multi-scale surface textured micro pillar array (Fig. 6c). The 80 nm thick FC polymer was then deposited on the replicated multi-scale surface textured PDMS

micro pillar array to enhance the lyophobicity (Fig. 6d). Fig. 7 shows the SEM image of multi-scale surface textured PDMS micro pillar arrays.

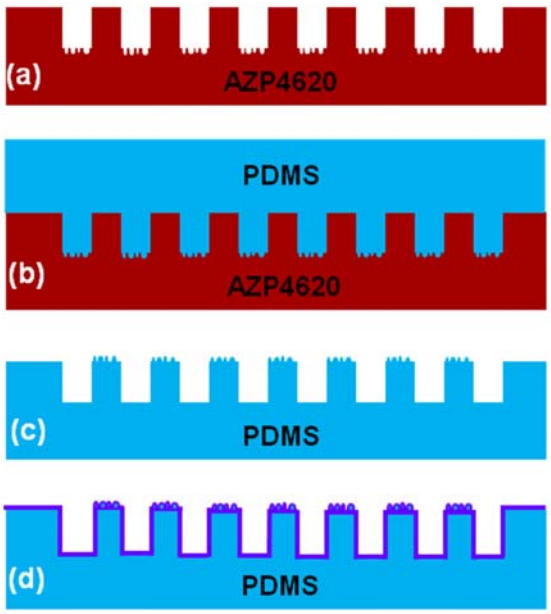

Fig. 6. Fabrication sequence of the multi-scale surface textured PDMS micro pillars: (a) fabrication of AZP4620 mold with multi-scale textures (under-baked and under-exposed), (b) PDMS casting, (c) replicated PDMS, (d) FC polymer deposition on the replicated multi-scale surface textured PDMS micro pillars.

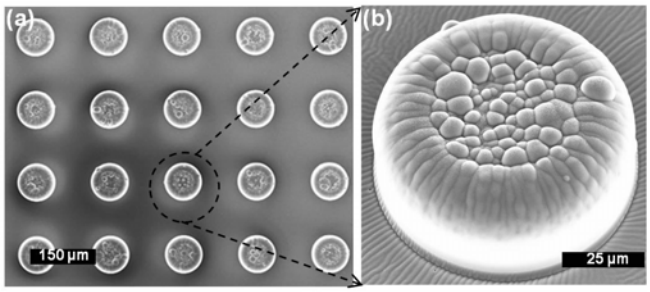

Fig. 7. SEM images of (a) multi-scale surface textured PDMS micro pillar arrays and (b) close-up view of a single pillar that is textured with additional roughness.

The static and dynamic contact angles were studied on the multi-scale PDMS micro pillar arrays for the naturally oxidized Galinstan® droplet. Fig. 8 shows static contact angles as a function of pitch distance in the range of 50 ~ 225 μm for the multi-scale PDMS micro pillar arrays as well as PDMS micro pillar and ridge arrays.

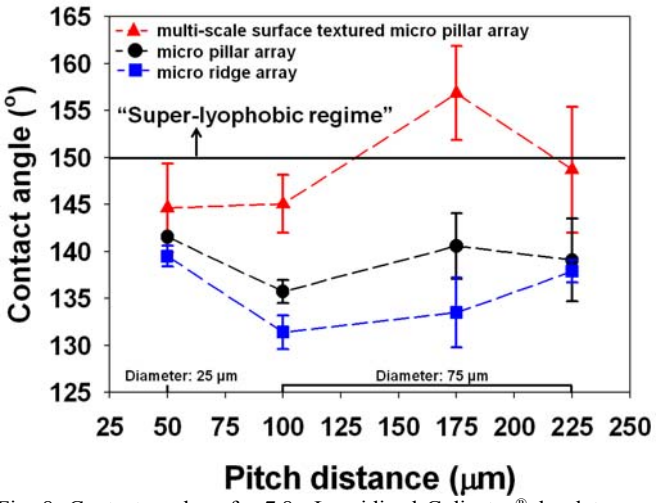

Fig. 8. Contact angles of a 7.8 μL oxidized Galinstan® droplet on a multi-scale surface textured micro pillar array, micro pillar and ridge arrays.

The static contact angle of the Galinstan® droplet on the FC polymer-deposited flat PDMS surface was 125.4º. The contact angle on the 100 μm pitch PDMS micro ridge array, on the other hand, was turned out to be 131.4º, showing only a small improvement in lyophobicity of the surface. However, the contact angle of the Galinstan® droplet on the multi-scale surface patterned PDMS micro pillar array was found to be substantially higher, to be close to the super-lyophobic regime (> 150º). 175 and 225 μm pitch distance multi-scale surface textured PDMS micro pillar arrays showed contact angles of 156.9º and 148.7º, respectively. Regardless of the pitch distance, the static contact angle on the multi-scale surface patterned micro pillar arrays is the highest compared to other textured surfaces. We believe that this is attributed to the lower solid fraction (f_s) based on the additional roughness of the multi-scale surface pattern on the micro pillar arrays. The solid fraction of the multi-scale surface textured micro pillar array cannot be directly calculated because the surface is irregularly patterned. Therefore, the solid fraction of the multi-scale surface textured PDMS micro pillar array was estimated by comparing static contact angles of the micro pillar arrays to those of the multi-scale surface textured PDMS micro pillar arrays. The experimentally determined solid fraction of the 175 μm pitch distance multi-scale surface patterned micro pillar array is 0.105 which is much smaller than that of the micro ridge array (0.429) and of the micro pillar array (0.144).

Fig. 9a shows the advancing and receding contact angles as a function of solid fraction of micro pillar arrays, micro ridge arrays and multi-scale surface patterned micro pillar arrays. The advancing contact angles are larger than 150º for all micro arrays, but the receding contact angles varies drastically as a function of the solid fraction. Of various micro arrays, the 175 μm pitch distance (75 μm diameter pillar 100 μm gap) multi-scale surface patterned PDMS micro pillar arrays showed the largest advancing and receding contact angles of approximately 175º and 163º (Fig. 10a and b), respectively. Fig. 9b shows the contact angle hysteresis as a function of the solid fraction for various micro arrays. The contact angle hysteresis increases as the solid fraction increases. The smallest

contact angle hysteresis (12º) was obtained on the 175 μm pitch distance multi-scale surface patterned PDMS micro pillar array while the 100 μm pitch distance micro ridge array (X-direction) showed the largest contact angle hysteresis of 140º.

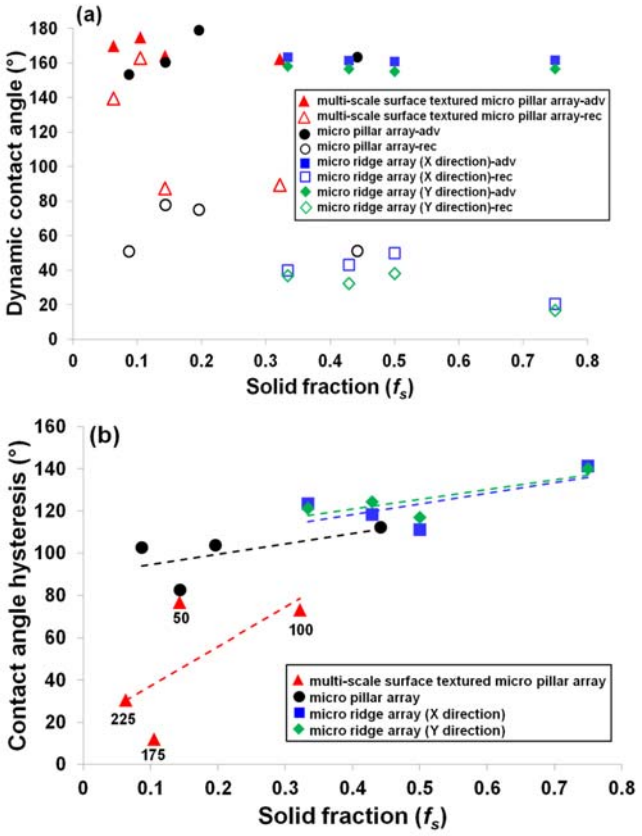

Fig. 9. (a) The measured advancing and receding contact angles, and (b) contact angle hysteresis of multi-scale surface patterned micro pillar arrays, micro pillar and ridge arrays as a function of solid fraction (numbers in the graph indicates pitch distance in μm). The colored dot lines are trend lines for multi-scale surface patterned micro pillar arrays, micro pillar and ridge arrays.

With the smallest contact angle hysteresis, we found that there remains no residue of oxidized Galinstan® after the droplet recedes from the surface (Fig. 10c) with the 175 μm pitch distance multi-scale surface patterned PDMS micro pillar array.

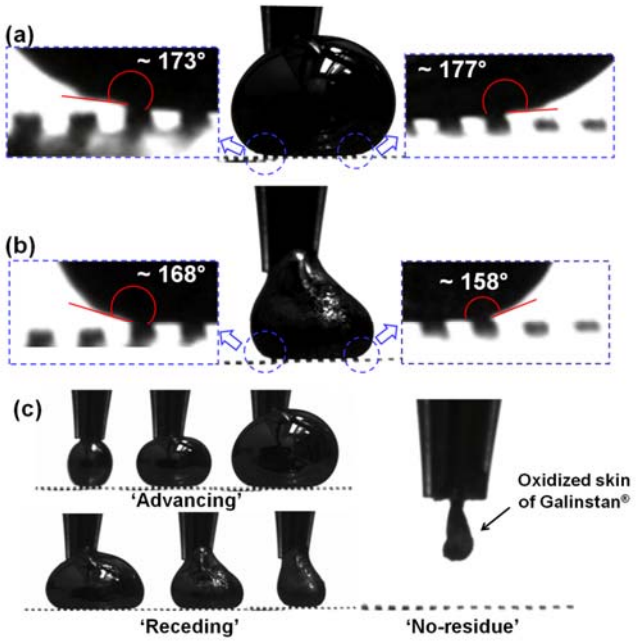

Fig. 10. Optical images of an oxidized Galinstan® droplet on the multi-scale surface patterned PDMS micro pillar arrays (pitch distance: 175 μm) during dynamic contact angle test: (a) advancing contact angle (θ_{adv} = 175°), (b) receding contact angle (θ_{rec} = 163°), and (c) evidence of no-residue after receding from the surface.

It should be noted that the contact angle hysteresis for the multi-scale surface textured PDMS micro pillar array (pitch distance 175 μm) for "oxidized" Galinstan® droplet was 12º which was smaller than the results obtained for "true liquid phase" Galinstan® in the < 1 ppm oxygen environment reported by Liu et al. [8]. With this encouraging result, we carried out further experiments to manipulate naturally oxidized Galinstan® droplets on the multi-scale surface textured PDMS micro pillar arrays by applying pressurized air on the droplets and found out that there was virtually no sign of residue despite the existence of natural oxide layer on the surface of Galinstan® droplets.

V. 3D SUPER-LYOPHOBIC CHANNEL AS A MICROFLUIDIC PLATFORM FOR OXIDIZED GALINSTAN® DROPLETS

As a logical next step, to develop a microfluidic platform for on-demand manipulation of the oxidized Galinstan®, we designed a simple microfluidic channel whose inner walls are patterned with multi-scale surface textured PDMS micro pillar array all around in 3D [25]. Fig. 11 shows the conceptual schematic diagram of the proposed fabrication procedure of the 3D super-lyophobic channel. Since PDMS is mechanically compliant, it is an ideal material for such a unique and simple microfluidic channel fabrication process.

For the fabrication of the 3D super-lyophobic channel, two pieces of multi-scale surface textured PDMS micro pillar array with 175 μm pitch distance were fabricated. On the both ends of the backside of one piece, oxygen plasma was treated (RF power of 50 W, pressure at 100 mTorr for 10 sec.) and glass slides were bonded (Fig. 11a). Then, glass slides were pushed inward to buckle the PDMS sheet and form inverse U-shape as shown in Fig. 11b; U-shaped PDMS surfaces later forms the top

part of the microfluidic channel. Next, the top PDMS sheet and the other PDMS sheet were plasma treated and bonded together (Fig. 11c). The bonded PDMS microfluidic channel was annealed in 110°C convection oven to improve the adhesion. The parabolic cross section of the channel was 2.2 mm wide and 3.2 mm high. Fig. 11d shows an optical image of the one end of the PDMS channel and Fig. 11e shows a Galinstan® droplet placed inside the microfluidic channel. It is evident from the shape of the droplet that the oxidized Galinstan® does not wet the surface of the micro-pillar surrounded channel. Repeated experiments on moving the oxidized Galinstan® droplet in the 3D microfluidic channel were carried out. Unlike other tested surfaces (flat surface, micro ridge array and micro pillar array), the oxidized Galinstan® droplet in the 3D channel did not leave any residue.

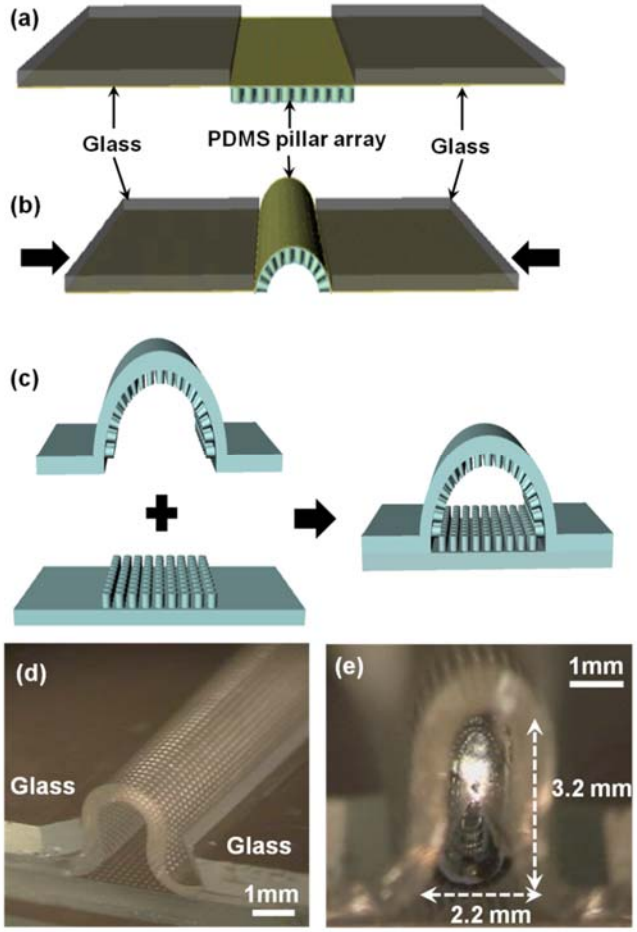

Fig. 11. Fabrication sequence of the super-lyophobic microfluidic channel: (a) glass slides attached on the two sides of the PDMS, (b) inverse U-shape PDMS channel formed, (c) PDMS-PDMS bonding to create the microfluidic channel platform. Optical images of (d) one end of the super-lyophobic PDMS channel and (e) Galinstan® droplet placed in the PDMS microfluidic 3D channel.

In order to quantify the minimum driving force to move a oxidized Galinstan® droplet in the fabricated 3D super-lyophobic microfluidic channel, centrifugal force measurements were carried out (Fig. 12). The centrifugal force (F_t) is given by:

$$F_t = mr\omega^2 \quad (3)$$

where m, r, and ω are the mass, the radial location, and the angular velocity of the droplet, respectively.

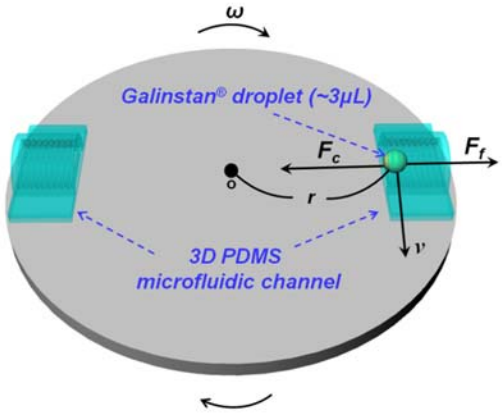

Fig. 12. Experimental setup of measuring centrifugal force of an oxidized Galinstan® droplet (~3μL) placed in the 3D PDMS microfluidic channel.

Two pieces of 1.5 cm long 3D PDMS microfluidic channels were taped down to a 4 inch diameter spin coater chuck, 1.6 cm and 0.8 cm away from the center, respectively. A ~3 μL droplet of naturally oxidized Galinstan® was placed at the end of the channel closer to the center of the spinning axis. The spin speed was ramped up with the rate of 100 rpm/sec. to the target spin speed and maintained for 10 seconds after it reached to the target spin speed. Table IV shows the results of the centrifugal force measurements. For the samples of 1.6 cm and 0.8 cm radial distances from the center, 975 rpm and 1280 rpm were the minimum spin speeds, respectively, for the movement of the oxidized Galinstan® droplet in the 3D PDMS microfluidic channel. Since the droplet moves only when the centrifugal force is greater than the adhesive force, it was determined that the minimum driving force for the movement of the naturally oxidized Galinstan® droplet in the 3D super-lyophobic microfluidic channel to be 3.11 ± 0.23 mN.

Table IV. Calculation of centrifugal force

	m (g)	r (cm)	spin speed (rpm)	w (rad/s)	a (m/s^2)	g-factor (a/g)	F (mN)
1	0.02	1.6	975	102.10	166.80	17.01	3.34
2	0.02	0.8	1280	134.04	143.84	14.66	2.88

VI. CONCLUSION

A study was carried out to understand the lyophobicity of various flat as well as textured surfaces with a goal of finding a super-lyophobic surface against the oxidized Galinstan®, and to demonstrate a microfluidic platform for on-demand manipulation of the oxidized Galinstan® droplet. Textured surfaces clearly showed improvement on the lyophobicity. The multi-scale surface textured PDMS micro pillar array with right solid fraction showed no evidence of surface wetting for the oxidized Galinstan® droplet. A simple procedure of fabricating a 3D super-lyophobic microfluidic channel structure was

demonstrated and on-demand movement of the oxidized Galinstan® was also demonstrated without any wetting residue left behind in the channel. This basic study shows one of the possible ways to overcome the nagging problems of the instant oxidation of gallium-based eutectic liquid metal alloy. We believe this result has a great potential to be utilized for many functional device demonstrations using gallium-based liquid metal alloy.

REFERENCES

[1] M. Knoblauch, *et al.*, "A galinstan expansion femtosyringe for microinjection of eukaryotic organelles and prokaryotes," *Nat Biotech,* vol. 17, pp. 906-909, 1999.

[2] P. Sen and K. Chang-Jin, "Microscale Liquid-Metal Switches : A Review," *Industrial Electronics, IEEE Transactions on,* vol. 56, pp. 1314-1330, 2009.

[3] W. Irshad and D. Peroulis, "A Silicon-Based Galinstan Magnetohydrodynamic Pump," in *PowerMEMS* Washington DC, USA, 2009, pp. 127-129.

[4] K.-Q. Ma and J. Liu, "Heat-driven liquid metal cooling device for the thermal management of a computer chip," *Journal of Physics D: Applied Physics,* vol. 40, p. 4722, 2007.

[5] W. Huaren, *et al.*, "Analysis of a Liquid Metal Current Limiter," *Components and Packaging Technologies, IEEE Transactions on,* vol. 32, pp. 572-577, 2009.

[6] L. Meng, *et al.*, "Liquid-Tunable Frequency Selective Surfaces," *Microwave and Wireless Components Letters, IEEE,* vol. 20, pp. 423-425, 2010.

[7] F. Scharmann, *et al.*, "Viscosity effect on GaInSn studied by XPS," *Surface and Interface Analysis,* vol. 36, pp. 981-985, 2004.

[8] L. Tingyi, *et al.*, "Characterization of Nontoxic Liquid-Metal Alloy Galinstan for Applications in Microdevices," *Microelectromechanical Systems, Journal of,* vol. 21, pp. 443-450, 2012.

[9] M. D. Dickey, *et al.*, "Eutectic Gallium-Indium (EGaIn): A Liquid Metal Alloy for the Formation of Stable Structures in Microchannels at Room Temperature," *Advanced Functional Materials,* vol. 18, pp. 1097-1104, 2008.

[10] D. Kim, *et al.*, "Recovery of Nonwetting Characteristics by Surface Modification of Gallium-Based Liquid Metal Droplets Using Hydrochloric Acid Vapor," *ACS Applied Materials & Interfaces,* vol. 5, pp. 179-185, 2013.

[11] H. Y. Erbil, *et al.*, "Transformation of a Simple Plastic into a Superhydrophobic Surface," *Science,* vol. 299, pp. 1377-1380, February 28, 2003 2003.

[12] T.-G. Cha, *et al.*, "Nanoscale Patterning of Microtextured Surfaces to Control Superhydrophobic Robustness," *Langmuir,* vol. 26, pp. 8319-8326, 2010/06/01 2010.

[13] N. J. Shirtcliffe, *et al.*, "Dual-Scale Roughness Produces Unusually Water-Repellent Surfaces," *Advanced Materials,* vol. 16, pp. 1929-1932, 2004.

[14] Z. Yoshimitsu, *et al.*, "Effects of Surface Structure on the Hydrophobicity and Sliding Behavior of Water Droplets," *Langmuir,* vol. 18, pp. 5818-5822, 2002/07/01 2002.

[15] C. G. L. Furmidge, "Studies at phase interfaces. I. The sliding of liquid drops on solid surfaces and a theory for spray retention," *Journal of Colloid Science,* vol. 17, pp. 309-324, 1962.

[16] D. Bodas and C. Khan-Malek, "Hydrophilization and hydrophobic recovery of PDMS by oxygen plasma and chemical treatment—An SEM investigation," *Sensors and Actuators B: Chemical,* vol. 123, pp. 368-373, 2007.

[17] T. Scharnweber, *et al.*, "Rapid prototyping of microstructures in polydimethylsiloxane (PDMS) by direct UV-lithography," *Lab on a Chip,* vol. 11, pp. 1368-1371, 2011.

[18] D. Fuard, *et al.*, "Optimization of poly-di-methyl-siloxane (PDMS) substrates for studying cellular adhesion and motility," *Microelectronic Engineering,* vol. 85, pp. 1289-1293, 2008.

[19] B. H. Jo, *et al.*, "Three-dimensional micro-channel fabrication in polydimethylsiloxane (PDMS) elastomer," *Microelectromechanical Systems, Journal of,* vol. 9, pp. 76-81, 2000.

[20] D. Quéré, "Rough ideas on wetting," *Physica A: Statistical Mechanics and its Applications,* vol. 313, pp. 32-46, 2002.

[21] W. Choi, *et al.*, "A modified Cassie–Baxter relationship to explain contact angle hysteresis and anisotropy on non-wetting textured surfaces," *Journal of Colloid and Interface Science,* vol. 339, pp. 208-216, 2009.

[22] Y. Yoon, *et al.*, "Surface modified nano-patterned SU -8 pillar array optically transparent super-hydrophobic thin film," *Journal of Micromechanics and Microengineering,* vol. 22, p. 035012, 2012.

[23] D. Quere, "Surface chemistry: Fakir droplets," *Nat Mater,* vol. 1, pp. 14-15, 2002.

[24] Y. Yoon, *et al.*, "One-step fabrication of optically transparent polydimethylsiloxane artificial lotus leaf film using under-exposed under-baked photoresist mold," in *Micro Electro Mechanical Systems (MEMS), 2012 IEEE 25th International Conference on*, 2012, pp. 301-304.

[25] D. Kim, *et al.*, "A super-lyophobic PDMS micro-tunnel as a novel microfluidic platform for oxidized Galinstan®," in *Micro Electro Mechanical Systems (MEMS), 2012 IEEE 25th International Conference on*, 2012, pp. 1005-1008.

Daeyoung Kim received B.S degree in Electrical Engineering from Korea Military Academy, Seoul, Korea, in 2003. As a signal officer, he has served the Korea army since 2003. He received the M.S degree in Electrical Engineering from Wayne State University, Detroit in 2007. Since that time, he worked as a full time instructor at KAAY (Korea Army Academy at Yeong-Cheon). Now, he is currently pursuing the Ph.D. degree in The University of Texas at Dallas, Richardson, Texas. His research focuses on the lyophobic surfaces, microfluidics, and frequency selective surfaces using liquid metal.

Dong-Weon Lee received the Ph.D. degrees in Mechatronics engineering from Tohoku University, Sendai, Japan, in 2001. He has been a Professor of Mechanical Systems Engineering at Chonnam National University (CNU), South Korea since March of 2004. Previously, he was with the IBM Zurich Research Laboratory in Switzerland, working mainly on microcantilever devices for chemical AFM applications. At CNU, his research interests include smart cantilever devices, miniaturized energy harvester, smart structures, and nanoscale transducers.
Dr. Lee is a member of the technical program committee of IEEE Sensors Conference, Transducers, and Microprocesses and Nanotechnology Conference (MNC).

Wonjae Choi received the B.S. and M.S. degrees in mechanical engineering from Seoul National University in Korea, and obtained the Ph.D. degree in mechanical engineering from the Massachusetts Institute of Technology in 2009. Since then he worked as a postdoctoral research fellow at Harvard University, until he joined the University of Texas at Dallas in 2011. He is currently an Assistant Professor in the Department of Mechanical Engineering in the same university. His current research interests include microfluidics, multi-phase fluid mechanics, as well as surface wettability.

Jeong-Bong (JB) Lee (S'92–M'98–SM'08) received the B.S. degree in electronics engineering from Hanyang University, Seoul, Korea, in 1986, and the M.S. and Ph.D. degrees in electrical engineering from the Georgia Institute of Technology, Atlanta, in 1993 and 1997, respectively.

During 1997-1998, he was a research engineer at Georgia Tech. During 1999-2001, he was an assistant professor at the Louisiana State

University, Baton Rouge, Louisiana. He then moved to UT Dallas in May, 2001 and he is currently a Full Professor in the Department of Electrical Engineering, The University of Texas at Dallas, Richardson, Texas. He is the director of the Micro/Nano Devices and Systems Laboratory. His current research interests include microelectromechanical systems and nanophotonics.

Dr. Lee was a recipient of a National Science Foundation CAREER Award in 2001. In 2007, Dr. Lee served as a member of the external review panel for the Microsystems Division, Sandia National Laboratories. Dr. Lee also served as an Executive Program Subcommittee Member for the Transducers 2011 and currently serves as a Program Committee Member for the Transducers 2013 and IEEE Sensors 2013.